Bioorganic & Medicinal Chemistry 21 (2013) 5233–5245

Contents lists available at SciVerse ScienceDirect

Bioorganic & Medicinal Chemistry

journal homepage: www.elsevier.com/locate/bmc

Antitumor properties of substituted (αE)-α-(1H-indol-3-ylmethylene)benzeneacetic acids or amides

Giuseppe Forte [a], Cosimo Gianluca Fortuna [b], Loredana Salerno [a], Maria N. Modica [a], Maria A. Siracusa [a], Venera Cardile [c], Giuseppe Romeo [a], Alessandra Bulbarelli [d], Elena Lonati [d], Valeria Pittalà [a,*]

[a] Dipartimento di Scienze del Farmaco, Università degli Studi di Catania, viale A. Doria 6, 95125 Catania, Italy
[b] Dipartimento di Scienze Chimiche, Università di Catania, viale A. Doria 6, 95125 Catania, Italy
[c] Dipartimento di Scienze Bio-Mediche Sezione di Fisiologia, Università degli Studi di Catania, viale A. Doria 6, 95125 Catania, Italy
[d] Dipartimento di Scienze della Salute, Università degli Studi di Milano Bicocca, Via Cadore 48, 20900 Monza, Italy

ARTICLE INFO

Article history:
Received 11 January 2013
Revised 17 May 2013
Accepted 12 June 2013
Available online 27 June 2013

Keywords:
Prostate cancer
Indoles
Perkin–Oglialoro reaction
Retinoblastoma protein
$p21^{Cip1}$
DU145 cell line
DFT
VolSurf+

ABSTRACT

A novel class of indole derivatives characterized by a (αE)-α-(1H-indol-3-ylmethylene)benzeneacetic acid or amide scaffold was synthesized. These derivatives, assayed for cell-growth inhibition activity against a panel of six different tumor cell lines, showed strong antiproliferative activity and selectivity mainly towards DU145 cell line. In particular, compounds **2d**–**m** and **5** stand out for their cell growth inhibitory activity and, among them, compound **2d** emerged for its selectivity towards DU145 with respect to other tested tumor cell lines. DU145 treated with 1 μM of **2d** for 72 h showed $p21^{Cip1}$ induction and suppression of Akt signaling together with induction of Rb. From a computational point of view, two different approaches were used in order to study topology and electronic properties of the novel compounds and to shed light on their drug-likeness properties. Firstly, topological and electronic features of the compounds endowed with the most relevant biological activity were deepened; in parallel, some ADME properties like solubility and permeability were predicted.

1. Introduction

It is well known that cell proliferation and progression through the cell cycle are governed by a series of checkpoint controls, otherwise referred to as restriction points which are regulated by different families of enzymes.[1,2] Transition from normal to pre-cancer and cancer cells is a result of multi-step accumulation of genetic and epigenetic modifications that disrupt these orderly processes changing its programming regulation. Mutations or deregulation of genes responsible for cell cycle, cellular growth and differentiation, such as growth factors, receptor or cytoplasmatic tyrosine kinases, serine/threonine kinases, regulatory GTPases, and transcription factors play a chief role in tumor development.[1–5] Oncogenes encoded by mutated genes do not possess important regulatory elements and their production and activation is uncontrolled. Thereby, it becomes clear that mechanisms that trigger the process of carcinogenesis are many and complex. Several cytotoxic drugs (e.g. doxorubicin and camptotecin) result to an indirect, a specific block of the cell cycle and thus produce an irreversible damage to both normal and tumor cells with significant toxicity and side effects. Thereby, compounds able to specifically target tumor cells, leading to tumor cell arrest or apoptosis, with comparable efficacy but reduced toxicity would be desirable. However, in spite of our growing knowledge of the molecular biology of cancer, the success rate of new therapies directly targeting tumor-causing proteins remains unsatisfactory with few exceptions (e.g. the use of imatinib in chronic myelogenous leukemia).[6] One major obstacle is that the complexity and redundancy of signal transduction pathways have only been partially elucidated; secondly, high heterogeneity of tumor cells and high heterogeneity of cancers make unlikely that hitting a single target will result in therapeutically useful effects. Thus, it appears clear the needs for anticancer drugs with novel structures which, even if the mechanism of action is not completely elucidated, can effectively block the uncontrolled cell proliferation under tumor diseases.[7–9]

As a part of our work towards the development of novel agents endowed with antitumor activity,[10–13] we previously reported the synthesis of 1H-pyrrolo[2,3-b]pyridine derivatives (Fig. 1, general formula **1a**) and their use as therapeutic agents in the treatment of cancer and cell proliferative disorders.[14] We now report the synthesis, characterization, and *in vitro* antiproliferative activity against a panel of six human tumor cell lines of new

* Corresponding author. Tel.: +39 095 7384269; fax: +39 095 222239.
E-mail address: vpittala@unict.it (V. Pittalà).

0968-0896/$ - see front matter © 2013 Elsevier Ltd. All rights reserved.
http://dx.doi.org/10.1016/j.bmc.2013.06.030

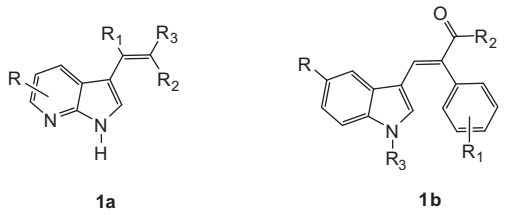

Figure 1. General chemical structure of **1a** and **1b**.

indole-derivatives differently substituted (Fig. 1, general formula **1b**). These classes of compounds, **1a** and **1b**, contain an **a**–**b** unsaturated ketone function which behaves as Michael reaction acceptors able to react with thiol groups present in proteins and glutathione. Interestingly, and perhaps not merely by coincidence, compounds with this structure are widely distributed in nature and have been reported to display a wide variety of pharmacological properties, for example, anticancer, antioxidant, antimutagenic activities, etc. Thus the inclusion of this substructure in our molecules can be regarded as a privileged structure able to recognize common key features present in biological systems.

Moreover, it was performed a computational study predicting some of their physico-chemical properties,[15] like adsorption, distribution, metabolism, excretion (ADME) properties, for verifying their applicability as potential drugs.

Furthermore, by means of a first principle approach, based on the Density Functional Theory (DFT), we studied topology and electronic properties, in terms of atomic charge values, of the compounds with relevant biological activity in order to localize the most reactive region of the molecules which will be candidate to interact with the biological substrate. The contribute due to intramolecular H-bond was also evaluated. Finally, some efforts have been made to elucidate the effect of lead compound on different intracellular pathways.

These computational and biological studies were performed to deepen the knowledge of the physico-chemical properties of the class in order to support, in the future, a more focused expansion of these derivatives and, hopefully, to discern their mechanism of action.

2. Chemistry

Novel derivatives **2c**–**m**, **3c**–**d**, **4a**–**d** and **5** were synthesized as reported in Scheme 1 and the synthetic route follows a strategy similar to the one used for the preparation of compounds **2a**, **2b**, **3a**, and **3b** previously reported.[16] Briefly, the first step of the synthetic pathway was focused on the preparation of (α*E*)-α-[1-acetyl-5-(phenylmethoxy)-1*H*-indol-3-ylmethylene]-benzeneacetic acids (**2c**–**m**), following the Perkin-Oglialoro reaction. It is known from literature data[16] that using this synthetic method, the main and usually the sole product has the (*E*)-config-

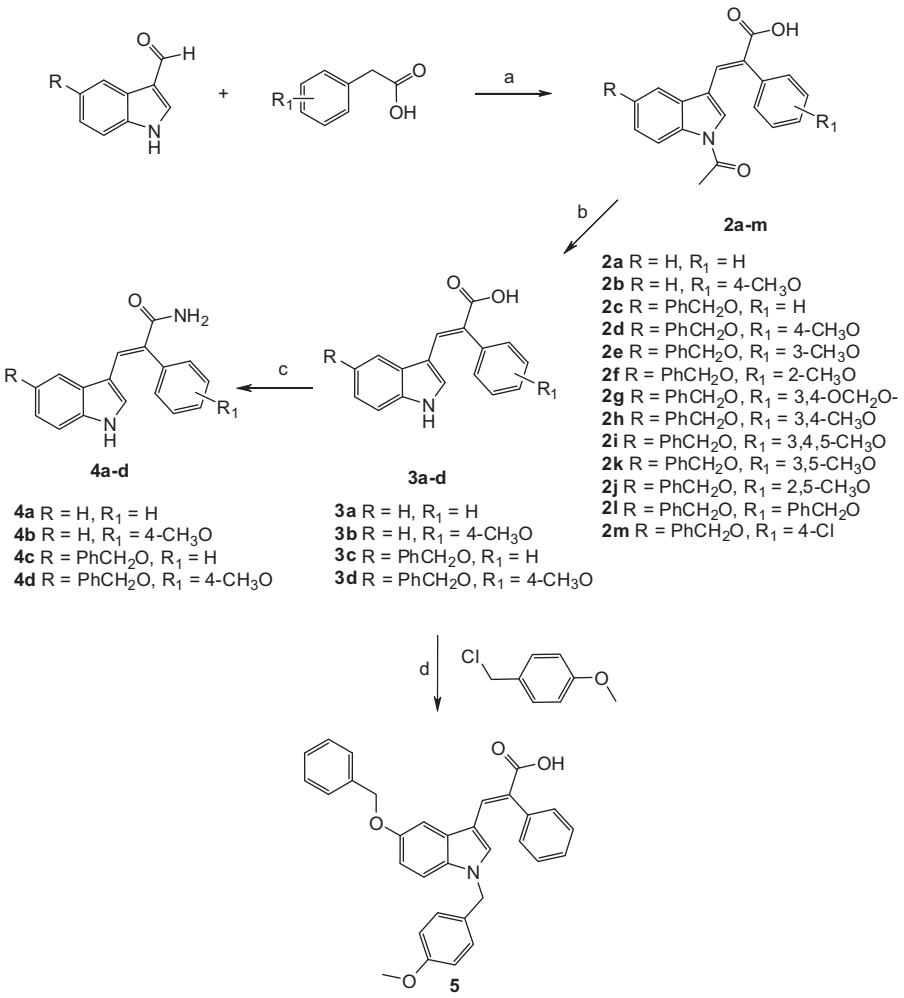

Scheme 1. Reagents and conditions: (a) TEA, acetic anhydride, 130 °C, 6 h, then H_2O/EtOH/THF (1:1:1); (b) NaOH 2 N, EtOH/THF (2:1), 70 °C, 1 h; (c) EDAC, HOBt·NH_3, TEA, DMF dry, 22 °C, 24 h; (d) NaH 95%, DMF dry, 22 °C, 24 h.

Table 1
In vitro activity of substituted (α*E*)-α-(1*H*-indol-3-ylmethylene)benzeneacetic acids or amides **2c–m**, **3a–d**, **4a–d**, and **5**

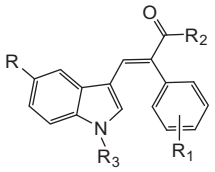

Compd	R	R_1	R_2	R_3	IC_{50} (μM)					
					DU145	LnCap	KB	A549	M14	Caco2
2c	$PhCH_2O$	H	OH	$COCH_3$	26.7	>100	55.5	57.5	>100	NT
2d	$PhCH_2O$	4-CH_3O	OH	$COCH_3$	0.91	85.0	>100	>100	>100	NT
2e	$PhCH_2O$	3-CH_3O	OH	$COCH_3$	1.08	65.1	>100	45.2	>100	NT
2f	$PhCH_2O$	2-CH_3O	OH	$COCH_3$	1.01	48.5	>100	57.2	>100	NT
2g	$PhCH_2O$	3,4-OCH_2O-	OH	$COCH_3$	1.15	99.1	>100	53.6	>100	NT
2h	$PhCH_2O$	3,4-CH_3O	OH	$COCH_3$	1.05	>100	96.7	54.8	65.5	NT
2i	$PhCH_2O$	3,4,5-CH_3O	OH	$COCH_3$	0.95	59.6	>100	89.1	57.1	NT
2k	$PhCH_2O$	3,5-CH_3O	OH	$COCH_3$	0.88	26.1	30.4	26.0	94.0	NT
2j	$PhCH_2O$	2,5-CH_3O	OH	$COCH_3$	0.83	44.1	>100	54.5	87.1	NT
2l	$PhCH_2O$	4-$PhCH_2O$	OH	$COCH_3$	1.41	77.7	43.0	44.1	58.2	NT
2m	$PhCH_2O$	4-Cl	OH	$COCH_3$	1.13	>100	>100	52.3	>100	NT
3a	H	H	OH	H	>100	NT	>100	NT	>100	>100
3b	H	4-CH_3O	OH	H	>100	NT	>100	NT	>100	>100
3c	$PhCH_2O$	H	OH	H	34.7	NT	55.5	NT	95.2	41.6
3d	$PhCH_2O$	4-CH_3O	OH	H	38.1	NT	38.5	NT	58.4	>100
4a	H	H	NH_2	H	33.3	NT	>100	NT	45.4	>100
4b	H	4-CH_3O	NH_2	H	40.0	NT	86.2	NT	53.0	>100
4c	$PhCH_2O$	H	NH_2	H	30.9	NT	40.3	NT	>100	>100
4d	$PhCH_2O$	4-CH_3O	NH_2	H	39.8	NT	>100	NT	>100	>100
5	$PhCH_2O$	4-CH_3O	OH	(4-CH_3OPh)CH_2	0.86	38.2	97.0	1.0	64.5	NT

uration, as desired. Thus, on these bases, we assume an (*E*)-configuration for the new synthesized compounds.

Hydrolysis of the acetamide group in compounds **2a–d** was achieved by heating at 70 °C for 2 h in the presence of 6 equiv of NaOH 2 N and afforded derivatives **3a–d**.[17]

The synthesis of the primary amides **4a–d** was achieved by treating the appropriate carboxylic acid (**3a–d**) with 1-hydroxybenzotriazole ammonium salt in the presence of *N′*-(ethylcarbonimidoyl)-*N*,*N*-dimethyl-1,3-propanediamine (EDAC) and triethylamine (TEA).

The alkylation of the indole nitrogen was performed, in high yield, using NaH 95% in dry DMF and 4-methoxyphenylmethyl chloride giving the *N*-[(4-methoxyphenyl)methyl]derivative **5**. The presence of a free carboxylic acid residue did not interfere in this reaction step.

All the synthesized products were characterized by ^1H NMR spectra, IR, and elemental analysis and data were consistent with the proposed structures.

3. Biology

These novel synthesized compounds were assayed for cell-growth inhibition activity at the concentrations of 1, 25, 50, and 100 μM for 72 h towards DU145 (human androgen-insensitive prostate cancer cells), LNCaP (human androgen-responsive prostate cancer cells), A549 (human bronchoalveolar carcinoma-derived cells), KB (human epidermoid cells), M14 (human melanoma cells), Caco2 (human intestinal epithelial cancer cells), and nontumorigenic human fibroblasts. Interestingly, for the latter, the values of percent viability of treated samples versus untreated controls were from 85% to 100%, indicating that new derivatives are not cytotoxic against normal cells. Data evaluation are summarized in Table 1 and are expressed as the concentration at which the tested compound reduces cell survival to 50% of the control value (IC_{50}). Data reported in Table 1 pointed out that almost all the novel synthesized compounds exerted mild cell growth inhibitory activity against all tested cell lines with the exception of the androgen nonresponsive DU145 human prostate cancer cells on which title compounds showed very interesting results in term of IC_{50} and selectivity. As a general trend, derivatives bearing a phenylmethoxy substituent at the 5-position of the indole ring, namely **2c–m**, **3c–d**, **4c–d**, and **5**, afforded the most interesting results when compared with unsubstituted derivatives **3a–b** and **4a–b**. Among the subclass of 5-phenylmethoxysubstituted compounds, derivatives bearing an acetyl or a 4-methoxyphenylmethyl residue at the indole nitrogen, namely **2c–m** and **5**, exhibited a better anti-proliferative activity (compare **2c–m** and **5** versus **3c–d** and **4c–d**). Moreover, results in Table 1 suggested that an amide function is preferable to an acidic function for derivatives unsubstituted at the indole ring (**4a–b** vs **3a–b**), while IC_{50} values are comparable when it is present a phenylmethoxy residue (**4c–d** vs **3c–d**). From IC_{50} values reported in Table 1 against tested tumor cell lines, compound **2d** stands out for its remarkable selectivity towards DU145, thus, it was selected as lead compound. These results are interesting because prostate cancer is the most common malignancy in men in a number of countries.[18,19] The incidence of prostate cancer has increased following the aging of population worldwide and, presently, conventional therapies such as surgery and hormone treatment frequently fail to achieve satisfactory effects.[20] The chance to develop new and more effective drugs for the treatment of prostate cancer remain an open opportunity and, in this light, we tried to elucidate the effect of lead compound **2d** on different intracellular pathways.

The serine/threonine protein kinase B (Akt) plays an important role in survival and proliferation of prostate cancer cells[21] and the extracellular signal-regulated protein kinases (Erk1,2) are critical regulators of growth and cell survival.[22] Hence, we investigated whether these cell signalings may play a role in survival and proliferation reduction observed in DU145 treated with 1 μM of **2d**

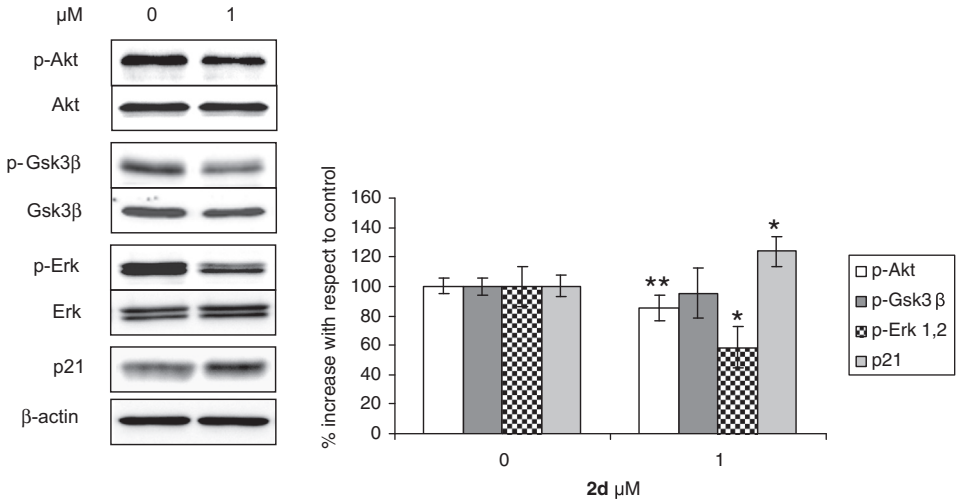

Figure 2. Effects of **2d** compound on cell survival and cell growth. DU145 cells incubated with 1 μM **2d** compound for 72 h were collected and lysed with 2% SDS lysis buffer. Equal amounts of samples (as protein content) were subjected to SDS–PAGE and western blot analysis. Phospho-Akt^{Ser473}, Akt, phospho-GSK3β Ser9, GSK3β, phospho-Erk1/2$^{Thr202/Tyr204}$, Erk1/2, p21, and β-actin levels were detected by specific antibodies, revealed by enhanced chemiluminescence (ECL) and semi-quantitatively estimated by Image Quant LAS 4000. Results obtained are shown on the bar-graphs. Anti-β-actin antibody was employed to confirm equal protein loading in the different lanes. Data represent the mean ± SEM of three separate experiments. Statistical significance is obtained with Student's *t* test in comparison with controls $^{*}p < 0.05$, $^{**}p < 0.01$.

for 72 h. Western blot analysis showed that levels of active phosphorylated-Akt^{Ser473} and -Erk1,$^{2Thr202/Tyr204}$ forms decreased in response to **2d** treatment about 20% and 40%, respectively. No effects were observed on steady-state levels of total Akt and Erk1,2 proteins (Fig. 2) as well as no significant change in Gsk3β phosphorylation state were observed after treatment given that **2d** seems to induce the decrease of Gsk3β protein level with respect to control (Fig. 2).

Moreover, in order to investigate **2d** compound effects on cell cycle, we assessed expression of p21^{Cip1} and cyclin-dependent kinase inhibitors that can complex with a variety of cyclins leading to cell cycle arrest. As shown in Fig. 2, treatment with 1 μM of **2d** resulted in p21^{Cip1} protein expression significant increase.

Taken together these data seems to be of interest since the reduction of Akt and Erk1,2 activity might influence the FOXO transcriptional activity,[23] involved in regulation of p21^{Cip1} expression.[24]

Moreover, since p21^{Cip1} is responsible for inactivating the retinoblastoma protein (Rb),[25] some samples of DU145 cells were assayed for Rb (Fig. 3). The retinoblastoma protein (Rb) pathway represents a key component in the regulation of the cell cycle and tumor suppression possessing important roles in DNA replication during S phase and G2/M transition.[26] Phosphorylation modulates the activity of Rb that results inactive when phosphorylated. Here we show that, after **2d** compound treatment, the ratio of p-Rb (inactive)/Rb (active) forms decreases with respect to the control (Fig. 3) suggesting a potential involvement of Akt/ p21^{Cip1} pathway and suggesting an interesting hypothesis deserving future experiments.

Finally, to analyze the effect of a sub lethal dose of **2d** compound, the same experiments were also performed treating cells with 0.1 μM concentration, but no significant alterations were detected in the analyzed pathways (data not shown).

4. Computational studies

4.1. DFT calculations

Among the synthesized derivatives, seven compounds, namely **2d–f**, **2i–j** and **5**, were selected on the basis of their interesting IC_{50} values against DU145 cell line and ten structures for each of them were sampled by means of Molecular Dynamics (MD). These structures were subsequently, fully optimized in DFT approach, by using the Conductor-Like Polarizable Continuum Model (CPCM).

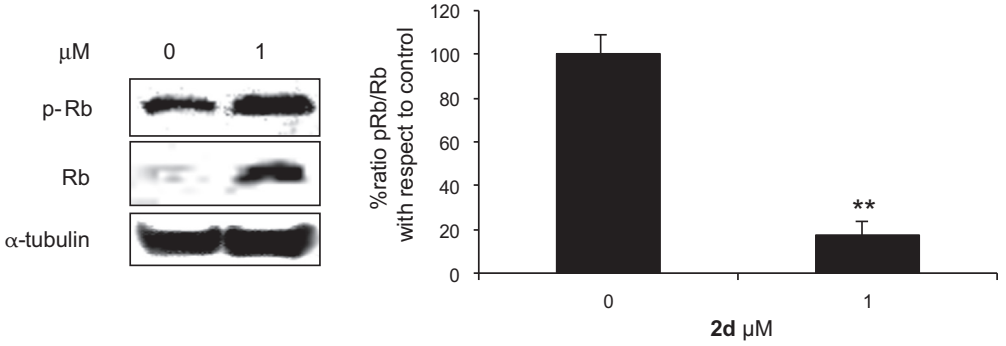

Figure 3. Effects of **2d** compound on Rb phosphorylation. DU145 cells incubated with 1 μM **2d** compound for 72 h were collected and lysed with 2% SDS lysis buffer. Equal amounts of samples (as protein content) were subjected to SDS–PAGE and Western blot analysis. Phospho-Rb$^{Ser249/Thr252}$, Rb and α-tubulin levels were detected by specific antibodies, visualized with autoradiography film. Bands were measured densitometrically and their relative density calculated based on the density of the α-tubulin band in each sample. Data represent the mean ± SEM of three separate experiments. Statistical significance is obtained with Student's *t* test in comparison with controls $^{**}p < 0.01$.

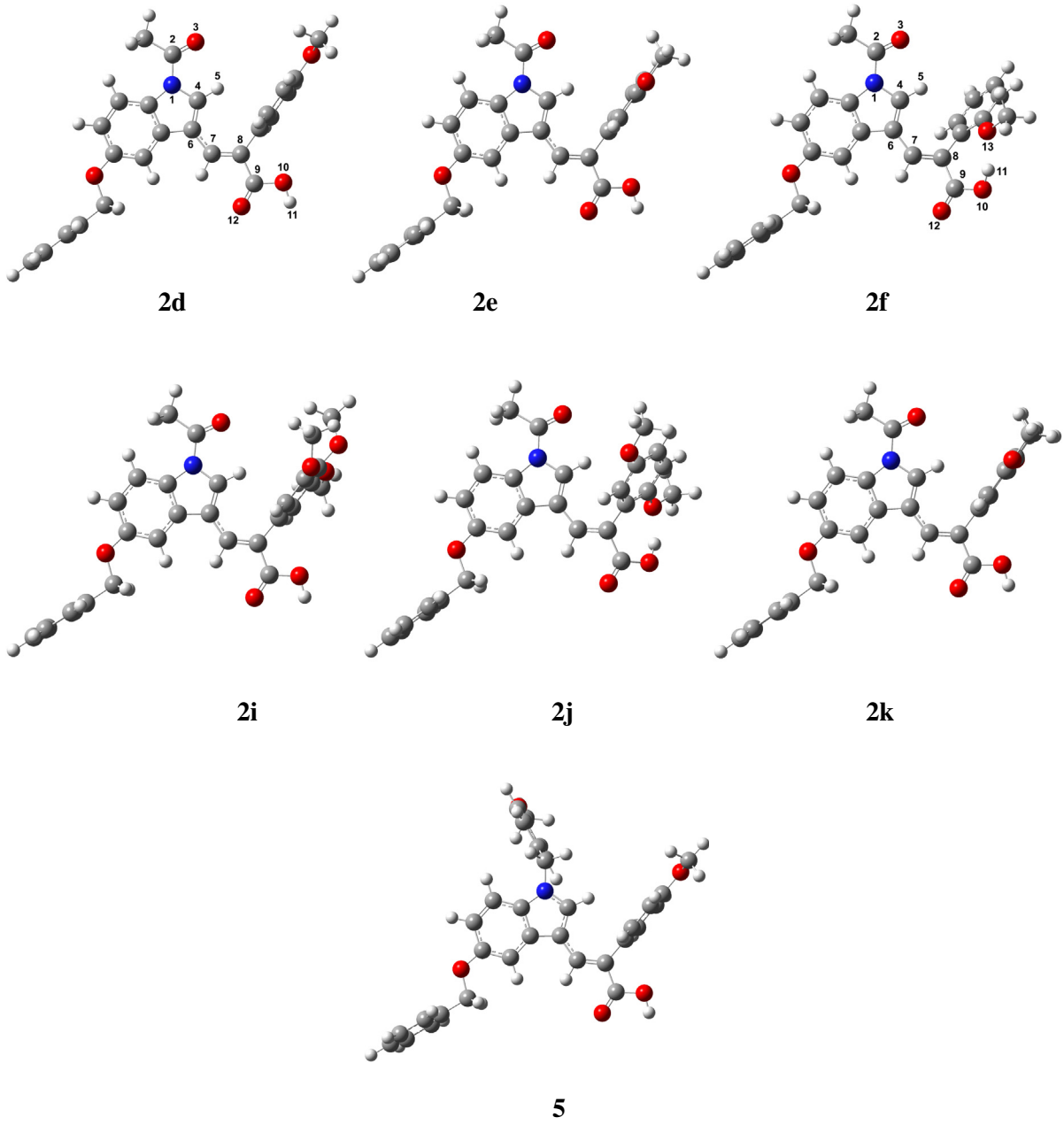

Figure 4. Lowest energy conformers, obtained after B3LYP/6-311+G** optimization, are reported below.

Such procedure gave rise to a scale of energy values of the different conformers; for the sake of clarity, in Fig. 4 we have reported the geometries lowest in energy. Nevertheless, it is to note that energy differences among the most part of the conformers are quite small (between 0.2–1 kJ/mol) and the standard deviation value (σ) for each configuration is less than 4. From a topological point of view we observe the presence of planar moieties in the molecules, due to an electron delocalization extended from the indole ring to the acidic group by means of conjugated double bonds (see Fig. 4 and bond order values reported in Table 2); nevertheless the topology of the phenyl ring substituted with different R_1 residues suggests us that binding DNA, through base pair intercalation, cannot occur since the steric hindrance due to the substituted phenyl ring. Atomic charge vales are also reported in Table 2. From these results we find out that the methoxyl groups, introduced as substituent in several position of the phenyl ring, play a main role only in terms of steric hindrance; in fact from an electronic point of view, effects induced by this group to the rest of the molecule are not appreciable (Table 2).

As to the position of the OCH_3 substituents, we observed only in 2-phenylsubstituted compounds, **2f** and **2j**, the formation of an intramolecular H-bond between the hydrogen atom of the carboxylic group and the oxygen atom of the methoxyl group. However, the amount of energy associated to this bond is estimated to be about 3 kJ/mol; due to this low energy value it is plausible that, at room temperature, vibrational modes break such weak bond making available the hydrogen of the carboxylic group to interact, by means of a H-bond, with the biological substrate.

From the electrostatic potential maps, reported in Fig. 5, one can distinguish the higher electron density area (in red) from the lower (in blue). As could be speculated looking at the chemical structures and as confirmed by these maps, it can be said that oxygen atoms in both carboxylic and amidic group can act as electron donors toward electrophilic groups of the substrate, on the other

Table 2
Wiberg bond order and atomic charges (a.u.) are reported for the main bonds and atoms. Numeration is referred to Fig. 4

BO	Charges (a.u.)	2d	2e	2f	2i	2j	2k	5	2f (COO^-)	2j (COO^-)
1–2		1.01	1.01	1.02	1.02	1.02	1.01	0.95	1.08	1.06
1–4		1.10	1.10	1.09	1.10	1.09	1.10	1.20	1.15	1.18
2–3		1.75	1.75	1.74	1.74	1.74	1.75	1.01	1.71	1.72
4–5		0.89	0.89	0.88	0.89	0.88	0.89	0.90	0.89	0.89
4–6		1.53	1.54	1.55	1.53	1.56	1.53	1.44	1.52	1.53
6–7		1.13	1.15	1.12	1.13	1.11	1.13	1.16	0.87	0.84
7–8		1.70	1.71	1.74	1.71	1.74	1.71	1.67	1.70	1.67
8–9		1.03	1.03	0.99	1.03	0.99	1.03	1.05	0.81	0.80
9–10		1.03	1.03	1.05	1.04	1.05	1.04	1.02	1.44	1.45
9–12		1.70	1.70	1.74	1.70	1.73	1.70	1.69	1.49	1.47
10–11		0.75	0.74	0.70	0.75	0.70	0.75	0.75	0.00	0.00
11–13		0.00	0.00	0.08	0.00	0.09	0.00	0.00	0.00	0.00
	1	−0.46	−0.45	−0.46	−0.46	−0.46	−0.47	−0.41	−0.53	−0.53
	2	0.71	0.71	0.71	0.71	0.71	0.71	−0.17	0.71	0.70
	3	−0.57	−0.57	−0.58	−0.58	−0.58	−0.57	–	−0.61	−0.58
	5	0.25	0.27	0.24	0.25	0.24	0.27	0.22	0.30	0.29
	10	−0.68	−0.68	−0.69	−0.68	−0.70	−0.68	−0.69	−0.77	−0.77
	11	0.48	0.49	0.49	0.49	0.49	0.49	0.48	0.00	0.00
	12	−0.63	−0.62	−0.59	−0.63	−0.59	−0.62	−0.65	−0.73	−0.74

hand the electrophilic hydrogen atom of the amidic group can form H-bond with heteroatoms, such as O or N, of the biological target.

It seems quite clear that the above considered compounds are pH sensitive and, at physiological pH, the carboxylate anion represents the predominate form. For this reason further geometry optimizations were carried out on the anionic species, starting from the neutral structures. Both topological and electronic modifications, with respect to the neutral form, are considerable only for compounds **2f** and **2j** and the related data are reported in Table 2. In these cases an electrostatic repulsion between the carboxylate and the substituent at the 2-position of the phenyl ring occurs. Anion structures, clearly, are strongly attracted by positive moieties present on the substrate; since the long-range character of the Coulomb force, electrostatic interaction could be considered the first recognition step with the active site of the substrate. Finally the marked anionic character of such compounds suggests a low affinity with the DNA.

4.2. VolSurf+ models

Several in silico methods were applied, in previous works,[27–29] reflecting both pharmacokinetic (PK) and pharmacodynamics (PD) aspect. In the present paper the PK profile of the database compounds was determined by use of the VolSurf+ software. VolSurf+ is an automatic procedure to convert 3D molecular fields into physico-chemical relevant molecular descriptors. VolSurf+ extracts the information present in 3D molecular field maps into few quantitative numerical descriptors, easy to understand and interpret. Molecular recognition is achieved coupling image analysis software with external chemical knowledge. Within this context, VolSurf+ selects molecular descriptors referred to molecular size and shape, to size and shape of both hydrophilic and hydrophobic regions and to the balance between them. Hydrogen bonding, amphiphilic moments, critical packing parameters are other useful descriptors. The VolSurf+ descriptors have been presented and explained in detail.[29] The originality of VolSurf+ resides in the fact that surfaces, volumes, and other related descriptors can be directly obtained from 3D molecular fields and can be used for multivariate model building to correlate the 3D molecular structures with biological behaviors.[30] The VolSurf+ methodology can also be applied for structure-activity relationships and molecular diversity based on surface properties. The selection of compounds with a favorable PK profile was guided by the projection on predefined models available in the VolSurf+ model library such as blood–brain barrier (BBB), absorption, solubility, metabolic stability.

In particular, we have taken into consideration the solubility in water and the intestinal absorption, two fundamental properties for the design of a potential drug useful for oral administration. The two properties are closely related because crossing the intestinal membrane requires a balance between hydrophilic and hydrophobic nature of the molecule. These two properties are orthogonal, that is, the increase of a property generally coincides with a decrease of the other. It is, therefore, important to obtain a high solubility in the aqueous phase but without reaching values that could lead to a decrease in intestinal absorption.

In Figs. 6–9 we report the PLS plot of the four models. The compounds used for the models are reported as black points and the projections of the synthesized compounds in yellow. The background are colored in basis of the activity; moving from red to blue zone the activity value increase.

Table 3 shows the quantitative values of solubility (Soly), intestinal permeability (Caco2), the permeability of the blood–brain barrier (BBB), and metabolic stability (MetStab).

On the basis of the range of properties of an optimal candidate reported in literature,[31] compounds **3a** and **3b** present the best solubility and metabolic stability but a low value of permeability. These values exclude **3a** and **3b** as lead compounds for further studies. On the other hand, compounds such as **2f**, **2d**, and **2g**–**2j** show a good compromise between the permeability and solubility and moderate good values for MetStab; thus these results could explain good *in vitro* antitumor activities of these derivatives.

5. Conclusions

In this report, a novel class of indole derivatives was described, synthesized with the aim of identifying novel compounds endowed with antitumor effects. These derivatives showed indeed strong antiproliferative activity against a panel of six human tumor cell lines, reaching IC_{50} values at submicromolar level. In particular, among synthesized derivatives, compounds **2d**–**m** and **5** stand out for their cell growth inhibitory activity and, particularly, compound **2d** emerged for its selectivity towards DU145 with respect to other tested tumor cell lines. Biological assays aimed at elucidating the effect of lead compound **2d** on different intracellular pathways led us to believe that $p21^{Cip1}$ induction and suppression of

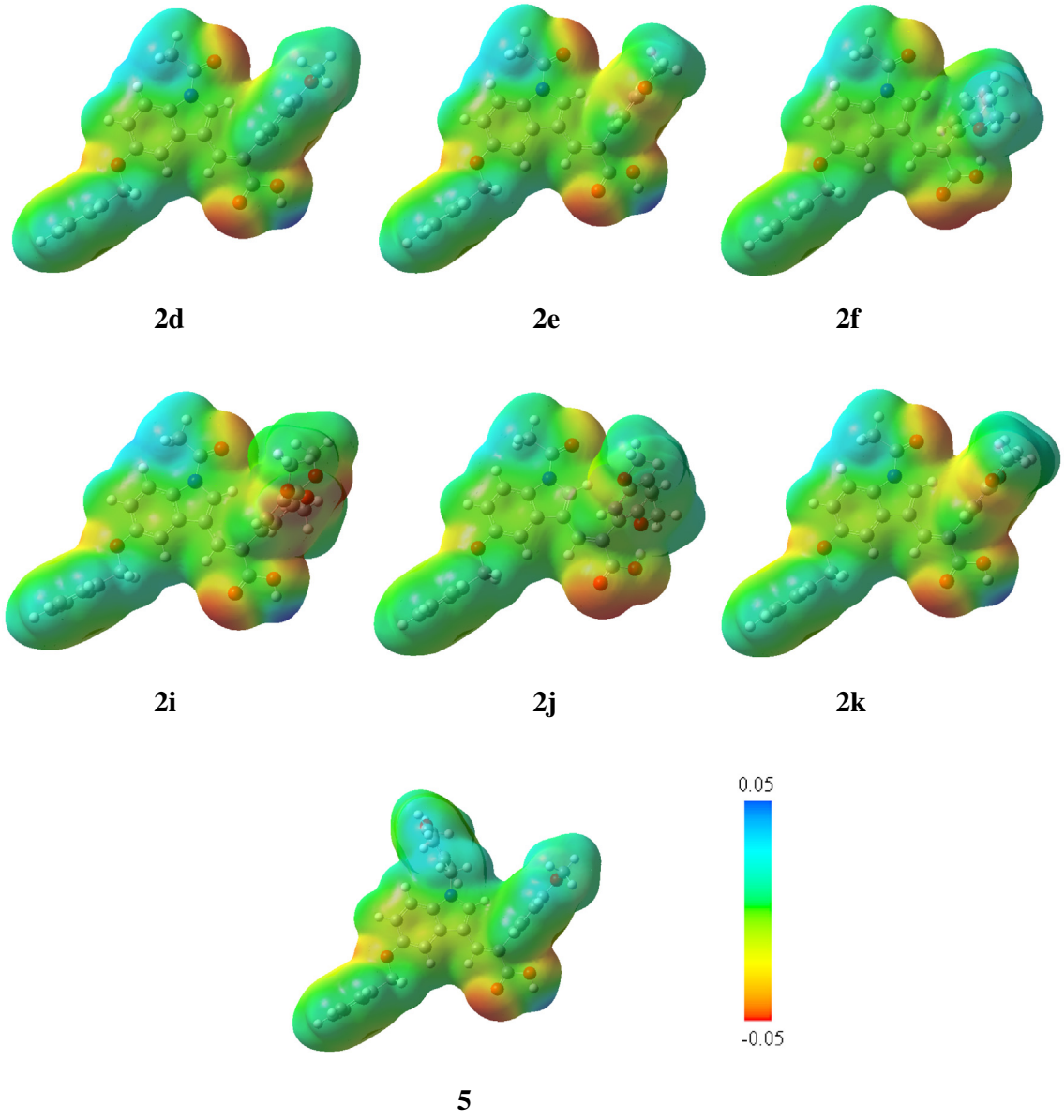

Figure 5. Electrostatic potential maps (e/A^3) are showed below. Blue color indicate regions with low electron density while red color is associated to high electron density moieties (see also the scale).

Akt signaling together with induction of Rb may play an important role in growth inhibition caused by **2d** treatment.

Two different computational approaches were used to better understand pharmacological profile of this new class on indole derivatives. These studies showed that, since their planar moieties, such compounds cannot act as DNA intercalators suggesting that other cellular molecular targets participate in the antiproliferative effect of compounds **2d**–**m** and **5**. Furthermore, the electron donor oxygen atom in amidic or carboxylic groups, can interact with moieties of amino acids in the biological substrate which, at physiological pH, act as 'H-bond donors' for example, Asn, Ser, Thr, Tyr. On the other hand, carboxylate anion is mainly involved in electrostatic interaction with positive charged area of the substrate which can be represented by basic amino acids such as His, Lys and Arg. It is to note that the absence of a remarkable positively charged group in the studied compounds give rise to a low affinity with DNA. A different biological activity of the derivatives can be ascribed to steric hindrance induced by OCH_3 substituent. Finally, we highlight that data emerged from the present work will help the future design of new potential and more active antitumor compounds that, while maintaining the indole ring, might present various substituents in different positions to improve the ADME properties, helping to clarify the mechanism of action of this novel class of indole derivatives.

6. Experimental procedures

6.1. Chemistry

Melting points were determined in a Electrothermal IA9200 apparatus with a digital thermometer in glass capillary tubes. Infrared spectra were recorded on a Perkin–Elmer FT IR 1600 spectrometer in KBr disks. Elemental analyses for C, H, and N were within ±0.4% of theoretical values and were performed on a Carlo Erba Elemental Analyzer Mod. 1108 apparatus. ^{1}H NMR spectra were recorded at 200 MHz on a Varian Inova Unity 200

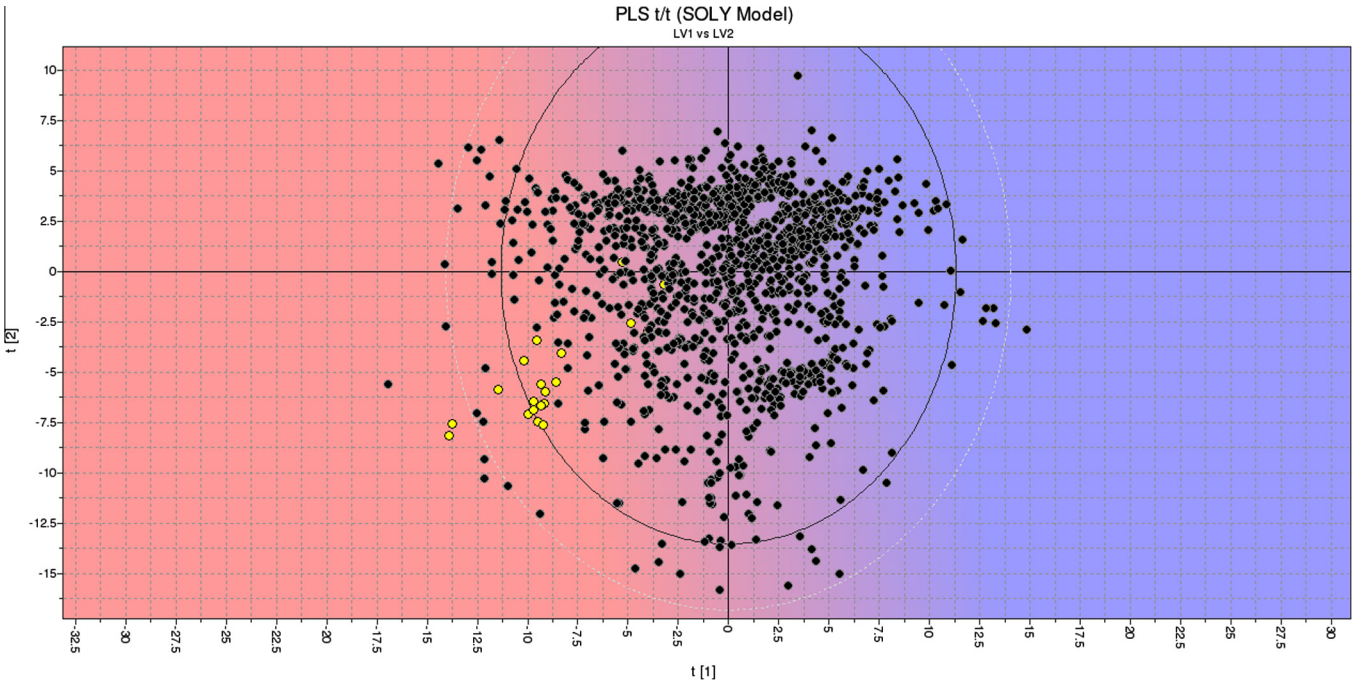

Figure 6. Soly model: the dots represent the molecules in the learning set (in black) and the synthesized compounds (in yellow).

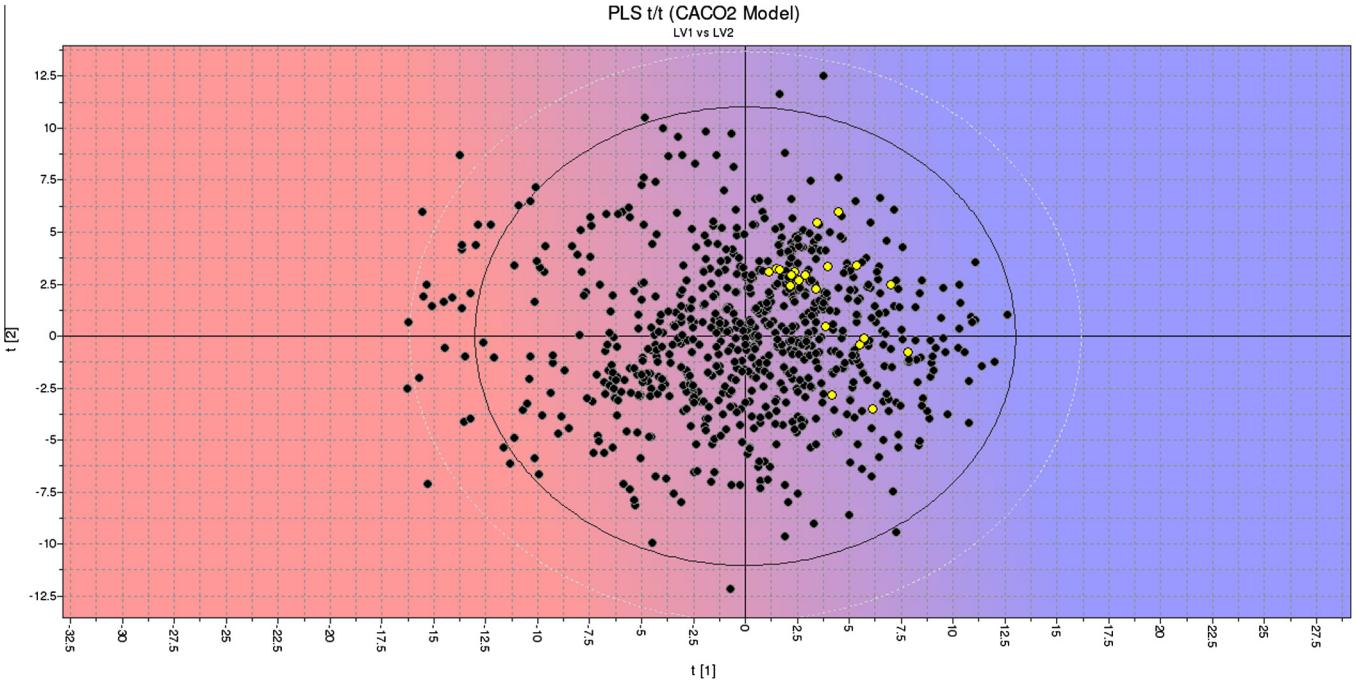

Figure 7. $CACO_2$ model: the dots represent the molecules in the learning set (in black) and the synthesized compounds (in yellow).

spectrometer in DMSO-d_6 solution. Chemical shifts are given in *d* values (ppm), using tetramethylsilane as the internal standard; coupling constants (*J*) are given in hertz (Hz). Signal multiplicities are characterized as s (singlet), d (doublet), t (triplet), q (quartet), m (multiplet), br (broad signal). All the synthesized compounds were tested for purity on TLC (aluminum sheet coated with silica gel F254, Merck) and visualized by UV (λ = 254 and 366 nm). All chemicals and solvents were of reagent grade and were purchased from commercial vendors. Compounds **2a**, **2b**, **3a**, and **3b** were synthesized as previously reported by the same authors.[16]

6.1.1. General procedure for the synthesis of (α*E*)-α-[[1-acetyl-5-(phenylmethoxy)-1*H*-indol-3-yl]methylene]substitutedbenzeneacetic acids (Method A) (2c, 2d, 2e, 2f, 2i, 2l, 2m)

A suspension of 5-(phenylmethoxy)-1*H*-indole-3-carboxaldehyde (0.500 g, 0.002 mol) and the appropriate phenylacetic acid (0.002 mol) in 1.88 mL of acetic anhydride (0.020 mol) and 0.277 mL of TEA (0.002 mol) was heated at 130 °C, for 6 h. The brown solution was cooled to 90 °C, 20 mL of H_2O/EtOH/THF (1:1:1) were added and the obtained mixture was vigorously stirred for 2 h, then allowed to cool at 22 °C and stirred for 14 h. The

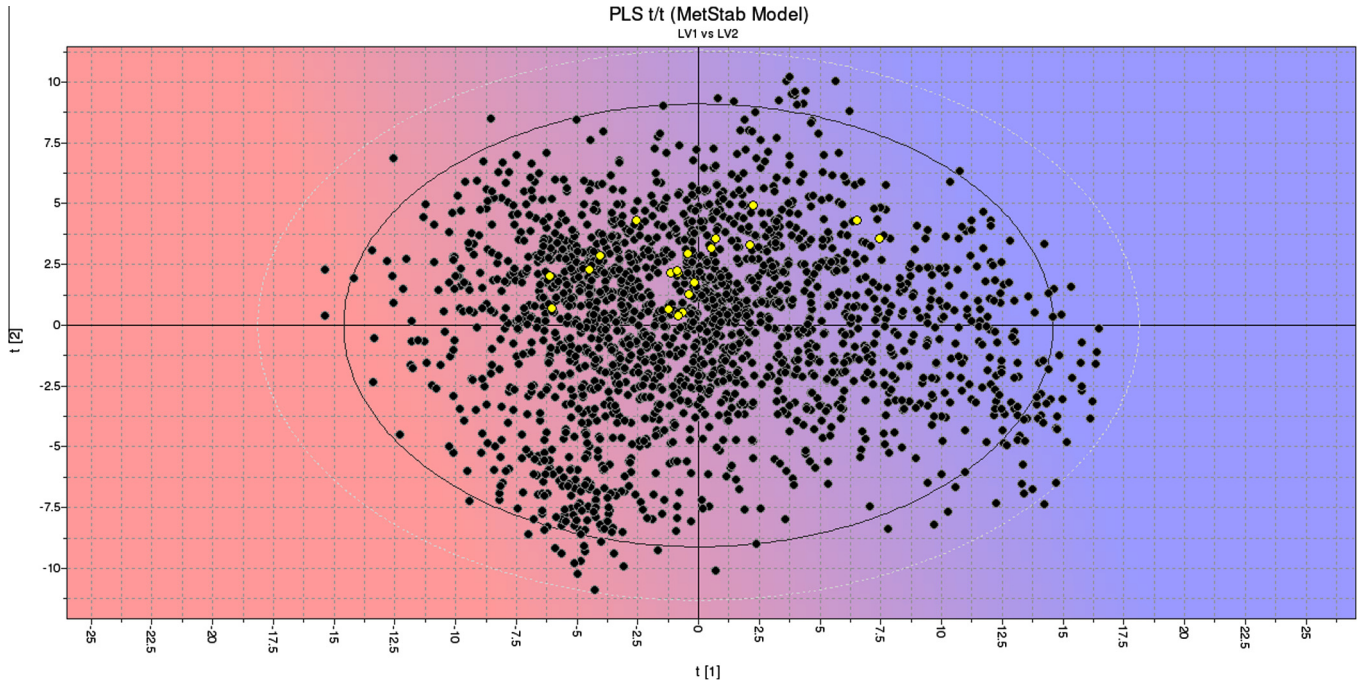

Figure 8. MetStab model: the dots represent the molecules in the learning set (in black) and the synthesized compounds (in yellow).

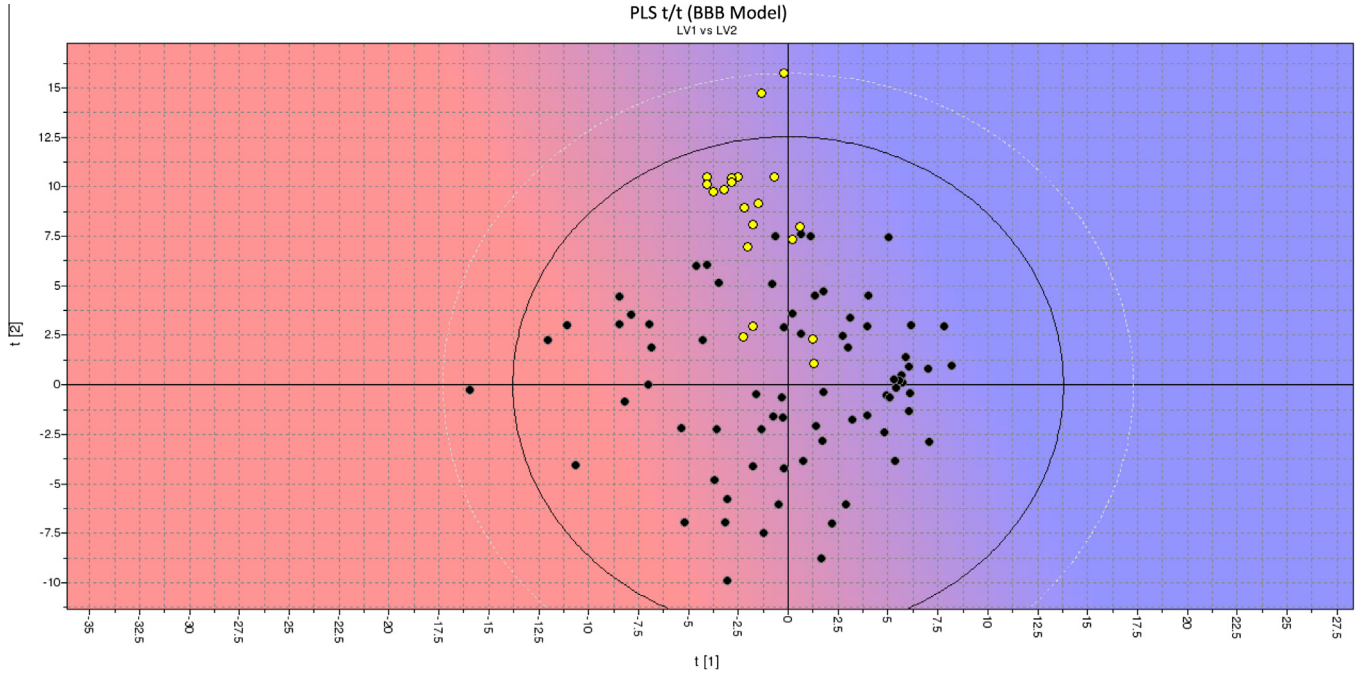

Figure 9. BBB model: the dots represent the molecules in the learning set (in black) and the synthesized compounds (in yellow).

obtained suspension was filtered and the solid was triturated in DCM/EtOH (3:7) to obtain the desired final product. Using this procedure the following compounds were obtained.

6.1.1.1. (α*E*)-α-[[1-Acetyl-5-(phenylmethoxy)-1*H*-indol-3-yl]methylene]benzeneacetic acid (2c). The title compound was obtained as a yellow powder (36%): mp 251–253 °C; IR (KBr) cm^{-1} 2932, 1706, 1667, 1587, 1458, 1385, 1280, 1254, 1221, 1013, 701; ^1H NMR (DMSO-d_6) d 8.16–8.09 (m, 1H, indole), 7.97 (s, 1H, C*H*═CCOOH), 7.54–7.23 (m, 10H, indole + aromatic), 7.10–7.00 (m, 2H, aromatic), 6.78 (s, 1H, NCH), 5.05 (s, 2H, CH_2), 2.23 (s, 3H, CH_3). Anal. ($C_{26}H_{21}NO_4$) C, H, N.

6.1.1.2. (α*E*)-α-[[1-Acetyl-5-(phenylmethoxy)-1*H*-indol-3-yl]methylene]-4-methoxybenzeneacetic acid (2d). The title compound was synthesized on a scale of 0.008 mol of starting materials and was obtained as a yellow powder (56%): mp 237–238 °C; IR (KBr) cm^{-1} 3564, 1700, 1513, 1456, 1390, 1223, 1168, 1032, 835; ^1H NMR (DMSO-d_6) d 12.65 (br s, 1H, COOH), 8.18–8.09 (m, 1H, indole), 7.92 (s, 1H, C*H*═CCOOH), 7.51–7.30 (m, 5H,

Table 3
Quantitative values of some pharmacokinetic properties obtained from the matrix of VolSurf+ descriptors

Measurements unit Compd	Log (Mol/L) SOLY	cm/s CACO2	Log (Mol/L) LgBB	% MetStab
2c	−5,46116	0.61832	−2,74298	46,3148
2d	−5,56853	0.55296	−2,91948	44,0852
2e	−5,57542	0.473478	−2,97634	43,9078
2f	−5,38938	0.519552	−2,86165	46,5748
2g	−5,40916	0.470385	−3,03668	47,7825
2h	−5,65412	0.388693	−3,12895	42,4053
2i	−5,51885	0.402218	−3,18018	42,0086
2j	−5,46909	0.489634	−2,97448	44,1951
2k	−5,42433	0.339976	−3,1804	45,1707
2l	−6,86235	0.623968	−2,7141	15,2722
2m	−6,11921	0.684529	−2,60381	34,7715
3a	−3,58103	0.950309	−2,27524	89,369
3b	−3,83048	0.712199	−2,78785	84,1348
3c	−5,15591	0.896818	−2,38646	52,5537
3d	−5,22823	0.675192	−2,78446	51,4396
4a	−4,22521	1,15193	−2,27003	61,0254
4b	−4,09877	0.87597	−2,87145	60,1342
4c	−5,52653	1,05687	−2,44954	26,6246
4d	−5,71983	0.852732	−2,83399	24,1309
5	−6,81326	0.748535	−2,52359	15,8121

indole + aromatic), 7.25–7.16 (m, 2H, aromatic), 7.06–6.90 (m, 5H, aromatic + NCH), 4.99 (s, 2H, CH_2), 3.76 (s, 3H, OCH_3), 2.32 (s, 3 H, CH_3). Anal. ($C_{27}H_{23}NO_5$) C, H, N.

6.1.1.3. (α*E*)-α-[[1-Acetyl-5-(phenylmethoxy)-1*H*-indol-3-yl]methylene]-3-methoxybenzeneacetic acid (2e). The title compound was synthesized on a scale of 0.008 mol of starting materials and was obtained as a yellow powder (47%): mp 224–226 °C; IR (KBr) cm^{-1} 1705, 1669, 1583, 1458, 1385, 1221, 1013, 798; ^1H NMR (DMSO-d_6) d 8.12–8.04 (m, 1H, indole), 7.95 (s, 1H, C*H*=CCOOH), 7.50–7.28 (m, 6H, indole + aromatic), 7.10–6.76 (m, 6H, aromatic + NCH), 5.02 (s, 2H, CH_2), 3.72 (s, 3H, OCH_3), 2.28 (s, 3H, CH_3). Anal. ($C_{27}H_{23}NO_5$) C, H, N.

6.1.1.4. (α*E*)-α-[[1-Acetyl-5-(phenylmethoxy)-1*H*-indol-3-yl]methylene]-2-methoxybenzeneacetic acid (2f). The title compound was obtained as a yellow powder (41%): mp 229–231 °C; IR (KBr) cm^{-1} 3018, 1699, 1690, 1460, 1390, 1252, 1218, 1163, 1022, 947, 755; ^1H NMR (DMSO-d_6) d 8.16–8.09 (m, 1H, indole), 7.91 (s, 1H, C*H*=CCOOH), 7.55–6.95 (m, 11H, indole + aromatic), 6.71 (s, 1H, NCH), 5.11 (s, 2H, CH_2), 3.72 (s, 3H, OCH_3), 2.23 (s, 3H, CH_3). Anal. ($C_{27}H_{23}NO_5$) C, H, N.

6.1.1.5. (α*E*)-α-[[1-Acetyl-5-(phenylmethoxy)-1*H*-indol-3-yl]methylene]-3,4,5-trimethoxybenzeneacetic acid (2i). The title compound was obtained as a light yellow powder (42%): mp 225–226 °C; IR (KBr) cm^{-1} 2939, 1705, 1582, 1503, 1456, 1385, 1240, 1124, 1006, 839; ^1H NMR (DMSO-d_6) d 8.11–8.20 (m, 1H, indole), 7.94 (s, 1H, C*H*=CCOOH), 7.50–7.33 (m, 5H, indole + aromatic), 7.07–6.93 (m, 3H, aromatic + NCH), 6.51–6.58 (m, 2H, aromatic), 5.04 (s, 2H, CH_2), 3.68 (s, 9 H, OCH_3), 2.34 (s, 3 H, CH_3). Anal. ($C_{29}H_{27}NO_7$) C, H, N.

6.1.1.6. (α*E*)-α-[[1-Acetyl-5-(phenylmethoxy)-1*H*-indol-3-yl]methylene]-4-phenylmethoxybenzeneacetic acid (2l). The title compound was obtained as a yellow powder (60%): mp 224–226 °C; IR (KBr) cm^{-1} 3061, 1702, 1687, 1610, 1512, 1458, 1383, 1250, 1222, 1013, 946, 829, 732; ^1H NMR (DMSO-d_6) d 8.17–8.11 (m, 1H, indole), 7.92 (s, 1H, C*H*=CCOOH), 7.40–6.89 (m, 17H, indole + aromatic + NCH), 5.10 (s, 2H, CH_2), 4.99 (s, 2 H, CH_2), 2.30 (s, 3H, CH_3). Anal. ($C_{33}H_{27}NO_5$) C, H, N.

6.1.1.7. (α*E*)-α-[[1-Acetyl-5-(phenylmethoxy)-1*H*-indol-3-yl]methylene]-4-chlorobenzeneacetic acid (2m). The title compound was obtained as a yellow powder (48%): mp 252–254 °C; IR (KBr) cm^{-1} 3061, 1702, 1689, 1456, 1388, 1260, 1223, 1167, 1031, 835, 731; ^1H NMR (DMSO-d_6) d 8.17–8.11 (m, 1H, indole), 7.99 (s, 1H, C*H*=CCOOH), 7.56–7.28 (m, 9H, indole + aromatic), 7.10–6.89 (m, 3H, aromatic + NCH), 4.99 (s, 2H, CH_2), 2.35 (s, 3H, CH_3). Anal. ($C_{26}H_{20}NO_4$) C, H, N.

6.1.2. General procedure for the synthesis of (α*E*)-α-[[1-Acetyl-5-(phenylmethoxy)-1*H*-indol-3-yl]methylene]substitutedbenzeneacetic acids (Method B) (2g, 2h, 2k, 2j)

A suspension of 5-(phenylmethoxy)-1*H*-indole-3-carboxaldehyde (0.500 g, 0.002 mol) and the appropriate phenylacetic acid (0.002 mol) in 1.88 mL of acetic anhydride (0.020 mol) and 0.277 mL of TEA (0.002 mol) was heated at 130 °C, for 6 h. The brown solution was cooled to 90 °C, 20 mL of H_2O/EtOH/THF (1:1:1) were added and the obtained mixture was vigorously stirred for 2 h, then allowed to cool at 22 °C and stirred for 14 h. The reaction mixture was concentrated, the residue diluted with water (50 mL) and extracted with CH_2Cl_2 (3 × 100 mL). The combined organic layers were dried over anhydrous Na_2SO_4, filtered, and evaporated. The obtained crude material was recrystallized from EtOH/CH_2Cl_2 (7:3) to obtain the desired final product. Using this procedure the following compounds were obtained.

6.1.2.1. (α*E*)-α-[[1-Acetyl-5-(phenylmethoxy)-1*H*-indol-3-yl]methylene]-1,3-benzodioxol-5-yl-acetic acid (2g). The title compound was obtained as a yellow powder (31%): mp 230–232 °C; IR (KBr) cm^{-1} 2893, 1705, 1690, 1608, 1541, 1453, 1381, 1236, 1036, 935, 700; ^1H NMR (DMSO-d_6) d 8.18–8.11 (m, 1H, indole), 7.92 (s, 1H, C*H*=CCOOH), 7.45–7.32 (m, 5H, indole + aromatic), 7.17–7.15 (m, 1H, aromatic), 7.02–6.85 (m, 4H, aromatic + NCH), 6.76–6.69 (m, 1H aromatic), 6.01 (s, 2H, OCH_2O), 5.02 (s, 2H, CH_2), 2.39 (s, 3H, CH_3). Anal. ($C_{27}H_{21}NO_6$) C, H, N.

6.1.2.2. (α*E*)-α-[[1-Acetyl-5-(phenylmethoxy)-1*H*-indol-3-yl]methylene]-3,4-dimethoxybenzeneacetic acid (2h). The title compound was obtained as a yellow powder (44%): mp 223–225 °C; IR (KBr) cm^{-1} 3060, 1705, 1674, 1513, 1452, 1387, 1257, 1218, 1145, 1021, 944, 696; ^1H NMR (DMSO-d_6) d 8.17–8.10 (m, 1H, indole), 7.92 (s, 1H, C*H*=CCOOH), 7.49–7.31 (m, 5H, indole + aromatic), 7.13–7.10 (m, 1H, aromatic), 7.05–6.74 (m, 5H, aromatic + NCH), 4.96 (s, 2H, CH_2), 3.75 (s, 3H, OCH_3), 3.66 (s, 3H, OCH_3), 2.35 (s, 3H, CH_3). Anal. ($C_{28}H_{25}NO_6$) C, H, N.

6.1.2.3. (α*E*)-α-[[1-Acetyl-5-(phenylmethoxy)-1*H*-indol-3-yl]methylene]-3,5-dimethoxybenzeneacetic acid (2k). The title compound was obtained as a yellow powder (50%): mp 244–245 °C; IR (KBr) cm^{-1} 2939, 1700, 1677, 1539, 1458, 1387, 1255, 1204, 1156, 1019, 945, 716; ^1H NMR (DMSO-d_6) d 8.13–8.06 (m, 1H, indole), 7.88 (s, 1H, C*H*=CCOOH), 7.41–7.30 (m, 5H, indole + aromatic), 7.04–6.96 (m, 3H, aromatic + NCH), 6.52–6.48 (m, 1H, aromatic), 6.39–6.35 (m, 2H, aromatic), 4.99 (s, 2H, CH_2), 3.65–3.61 (m, 6H, OCH_3), 2.28 (s, 3H, CH_3). Anal. ($C_{28}H_{25}NO_6$) C, H, N.

6.1.2.4. (α*E*)-α-[[1-Acetyl-5-(phenylmethoxy)-1*H*-indol-3-yl]methylene]-2,5-dimethoxybenzeneacetic acid (2j). The title compound was obtained as a yellow powder (33%): mp 200–202 °C; IR (KBr) cm^{-1} 3059, 1703, 1685, 1498, 1459, 1387, 1256, 1220, 1041, 947, 801; ^1H NMR (DMSO-d_6) d 8.17–8.10 (m, 1H, indole), 7.91 (s, 1H, C*H*=CCOOH), 7.48–7.35 (m, 5H, indole + aromatic), 7.24–7.20 (m, 1H, aromatic), 7.09–6.90 (m, 3H, aromatic), 6.81 (s, 1H, NCH), 6.72–6.67 (m, 1H, aromatic), 5.11 (s,

2H, CH_2), 3.69–3.62 (m, 6H, OCH_3), 2.27 (s, 3H, CH_3). Anal. ($C_{28}H_{25}NO_6$) C, H, N.

6.1.3. General procedure for the synthesis of (αE)-α-[[5-(phenylmethoxy)-1H-indol-3-yl]methylene]benzeneacetic acids (3c and 3d)

A solution of the appropriate (αE)-α-[[1-acetyl-5-(phenylmethoxy)-1H-indol-3-yl]methylene]benzeneacetic acid (**2c** or **2d**) (0.004 mol) in 12 mL of NaOH 2 N (0.024 mol), 12 mL of THF and 24 mL of ethanol was heated at 70 °C for 2 h. The obtained mixture was concentrated under reduced pressure, diluted with water. The aqueous layer was washed with DCM (1 × 50 mL), and acidified with HCl 37%. The obtained precipitate was filtered, dried and recrystallized from DCM/EtOH (1:1) to give the title compounds **3c** or **3d**.

Using this procedure the following compound was obtained.

6.1.3.1. (αE)-α-[[5-(Phenylmethoxy)-1H-indol-3-yl]methylene]benzeneacetic acid (3c). The title compound was obtained as a yellow powder (44%): mp 218–220 °C; IR (KBr) cm^{-1} 3375, 1669, 1587, 1453, 1416, 1272, 1193, 1107, 850, 737; ^1H NMR (DMSO-d_6) d 12.21 (br s, 1H, COOH), 11.41 (br s, 1H, NH), 8.06 (s, 1H, C*H*=CCOOH), 7.51–7.20 (m, 11H, indole + aromatic), 7.13–7.10 (m, 1H, aromatic), 6.88–6.78 (m, 1H, aromatic), 6.32 (d, *J* = 2.6 Hz, 1H, NCH), 5.07 (s, 2H, CH_2). Anal. ($C_{24}H_{19}N_2O_3$) C, H, N.

6.1.3.2. (αE)-α-[[5-(phenylmethoxy)-1H-indol-3-yl]methylene]-4-methoxybenzeneacetic acids (3d). The title compound was obtained as a yellow powder (71%): mp 180–182 °C; IR (KBr) cm^{-1} 3338, 1670, 1612, 1512, 1451, 1244, 1029, 743; ^1H NMR (DMSO-d_6) d 11.37 (br s, 1H, NH), 7.93 (s, 1H, C*H*=CCOOH), 7.49–6.73 (m, 12H, indole + aromatic), 6.43 (d, *J* = 2.6 Hz, 1H, NCH), 5.03 (s, 2H, CH_2), 3.77 (s, 3H, OCH_3). Anal. ($C_{25}H_{21}NO_4$) C, H, N.

6.1.4. General procedure for the synthesis of (αE)-α-[(5-substituted-1H-indol-3-yl)methylene]substitutetdbenzeneacetamide (4a–c)

A suspension of the appropriate carboxylic acid (0.5 mmol), TEA (1.2 mmol), and 1-hydroxybenzotriazole ammonium salt (1.0 mmol) in 1 mL of anhydrous DMF was cooled to 0 °C. EDAC (0.75 mmol) was added portion-wise and the reaction mixture was stirred for 24 h at 22 °C. The obtained mixture was diluted with ethyl acetate (100 mL) and the organic layer was separated and washed with water (2 × 50 mL), NaOH 1 N (1 × 50 mL), and brine (1 × 50 mL). The organic layer was dried over anhydrous Na_2SO_4, filtered, and evaporated. The obtained crude material was recrystallized from DCM to obtain the desired final product. Using this procedure the following compounds were obtained.

6.1.4.1. (αE)-α-[-(1H-Indol-3-yl)methylene]benzeneacetamide (4a). The title compound was obtained as a light yellow powder (73%): mp 187–189 °C; IR (KBr) cm^{-1} 3390, 2364, 1665, 1575, 1353, 1294, 1235, 749; ^1H NMR (DMSO-d_6) d 11.27 (br s, 1H, NH), 7.85 (s, 1H, C*H*=CCONH$_2$), 7.70–7.64 (m, 1H, indole), 7.58–7.02 (m, 8H, indole + aromatic), 6.63 (br s, 2H, NH_2), 6.08 (d, *J* = 2.6 Hz, 1H, NCH). Anal. ($C_{17}H_{14}N_2O$) C, H, N.

6.1.4.2. (αE)-α-[-(1H-Indol-3-yl)methylene]-4-methoxybenzeneacetamide (4b). The title compound was obtained as a light yellow powder (79%): mp 223–225 °C; IR (KBr) cm^{-1} 3163, 1640, 1547, 1513, 1366, 1232, 1139, 1034, 746; ^1H NMR (DMSO-d_6) d 11.25 (br s, 1H, NH), 7.84 (s, 1H, C*H*=CCONH$_2$), 7.72–7.64 (m, 1H, indole), 7.38–7.29 (m, 1H, indole), 7.20–7.01 (m, 6H, indole + aromatic), 6.53 (br s, 2H, NH_2), 6.17 (d, *J* = 2.6 Hz, 1H, NCH), 3.82 (s, 3H, OCH_3). Anal. ($C_{18}H_{16}N_2O_2$) C, H, N.

6.1.4.3. (αE)-α-[[5-(Phenylmethoxy)-1H-indol-3-yl]methylene]benzeneacetamide (4c). The title compound was obtained as a pale yellow powder (65%): mp 204–205 °C; IR (KBr) cm^{-1} 3353, 2364, 1657, 1567, 1480, 1379, 1190, 1002, 940, 745; ^1H NMR (DMSO-d_6) d 11.17 (br s, 1H, NH), 7.82 (s, 1H, C*H*=CCONH$_2$), 7.50–7.20 (m, 12H, indole + aromatic), 7.09 (br s, 1H, NH_2), 6.85–6.80 (m, 1H, aromatic), 6.65 (br s, 1H, NH_2), 6.08 (d, *J* = 2.6 Hz, 1H, NCH), 5.09 (s, 2H, CH_2). Anal. ($C_{24}H_{20}N_2O_2$) C, H, N.

6.1.4.4. (αE)-α-[[5-(Phenylmethoxy)-1H-indol-3-yl]methylene]-4-methoxybenzeneacetamide (4d). The title compound was obtained as a pale yellow powder (57%): mp 231–233 °C; IR (KBr) cm^{-1} 3164, 2364, 1659, 1568, 1479, 1241, 1021, 944, 803; ^1H NMR (DMSO-d_6) d 11.15 (br s, 1H, NH), 7.80 (s, 1H, C*H*=CCONH$_2$), 7.51–7.00 (m, 11H, indole + aromatic), 6.83–6.78 (m, 1H, aromatic), 6.51 (br s, 2H, NH_2), 6.22 (d, *J* = 2.6 Hz, 1H, NCH), 5.08 (s, 2H, CH_2), 3.80 (s, 3H, OCH_3). Anal. ($C_{25}H_{22}N_2O_3$) C, H, N.

6.1.5. (αE)-α-[[1-(4-Methoxyphenylmethyl)-5-(phenylmethoxy)-1H-indol-3-yl]methylene]benzeneacetic acid (5)

A solution of (αE)-α-[[5-(phenylmethoxy)-1H-indol-3-yl]methylene]-4-methoxybenzeneacetic acid (**3d**) (0.002 mol) in 5 mL of anhydrous DMF was cooled at 0 °C and 0.151 g of sodium hydride 95% (0.006 mol) were added. The obtained suspension was allowed to warm at 22 °C and stirred for 15 min. After this period, 4-methoxyphenylmethyl chloride (0.271 mL, 0.002 mol) in 1 mL of anhydrous DMF was added drop-wise and the obtained suspension was stirred at 22 °C for 24 h. The reaction mixture was slowly dropped in 70 mL of HCl 0.6 N. The obtained precipitate was filtered, dried and triturated from DCM/EtOH (1:1) to give the desired final product **5** as a light yellow powder (91%): mp 211–213 °C; IR (KBr) cm^{-1} 2929, 1663, 1612, 1514, 1250, 1175, 1023, 802; ^1H NMR (DMSO-d_6) d 7.97 (s, 1H, C*H*=CCOOH), 7.45–7.34 (m, 6H, indole + aromatic), 7.14–6.81 (m, 10H, aromatic), 6.54 (s, 1H, NCH), 5.10 (s, 2H, NCH_2), 5.03 (s, 2H, NCH_2), 3.77 (s, 3H, OCH_3), 3.72 (s, 3H, OCH_3). Anal. ($C_{33}H_{29}NO_5$) C, H, N.

6.2. Biological activity evaluation

6.2.1. Cell culture and treatments

DU145 and A549 cells were grown in Dulbecco's modified Eagle's medium (DMEM) containing 10% fetal calf serum (FCS), 100 U/mL penicillin, 100 mg/mL streptomycin, 1 mM glutamine, and 1% nonessential amino acids. LNCaP, KB and M14 cell lines were maintained in RPMI supplemented with 10% fetal calf serum, 100 U/mL penicillin, and 100 mg/mL streptomycin. Finally, Caco2 cells were maintained in minimum essential medium (MEM) supplemented with 10% fetal calf serum, 100 U/mL penicillin and 100 μg/mL streptomycin. All cultures were incubated at 37 °C within a humidified, 95% air and 5% CO_2 atmosphere. The medium was changed every 2 to 3 days. For the experiments the cells were plated at a constant density to obtain identical experimental conditions in the different tests, thus to achieve a high accuracy of the measurements. After 24 h incubation at 37 °C under a humidified 5% carbon dioxide to allow cell attachment, the culture medium was changed and the cells were treated with different concentrations (1, 25, 50, and 100 μM for 72 h) of new synthesised compounds.

6.2.2. Cell growth inhibition assay

To evaluate cell viability the MTT assay was employed: it measures the cellular capacity to reduce 3-(4,5-dimethylthiazol-2-yl)diphenyltetrazolium bromide to blue formazan products by

various mitochondrial dehydrogenase enzymes. Briefly, DU145, KB, M14, Caco2 cells and human adult fibroblasts (1×10^4) were set up in flat-bottomed 200 μL microplates, and incubated at 37 °C in a humidified 5% CO_2/95% air mixture for 24 h. Then, they were untreated (controls) or treated for 72 h with each experimental compound. Mother solutions of each derivative were prepared by dissolving it in the minimum amount of DMSO and after in culture medium. In each experiment, DMSO never exceeded 0.1%, and this percentage did not interfere with cell growth. All the compounds were tested at the concentrations of 1, 25, 50, and 100 μM. Four h before the end of the incubation period, 20 μL of 0.5% MTT in phosphate buffer saline was added to each microwell. After incubation with the reagent, the supernatant was removed and replaced with 100 μL DMSO. The optical density of each sample was measured with a spectrophotometer reader at λ = 550 nm. Three replicates were performed for each sample.

6.2.3. Western blotting analysis

Cells, submitted or not to treatments with **2d** compound for 72 h, were rinsed twice with phosphate-buffered saline (PBS), lysed in the presence of 2% SDS lysis buffer (50 mM Tris–HCl, pH 6.8, complete protease inhibitor Cocktail, plus the phosphatase inhibitors 2 mM Na orthovanadate, 1 mM NaF, 1 mM sodium pyrophosphate) harvested by scraping with a rubber policeman and quantified using Bicinchoninic acid assay (Pierce). Equal amount of total proteins were subjected to SDS–polyacrylamide electrophoresis on 10% gels, transferred to a nitrocellulose membrane (Amersham, GE Healthcare Europe GmbH, Milano, Italy) and proteins revealed by Ponceau staining (Sigma Chemical Co., Milano, Italy). Membranes were blocked in TBS-Tween 0.1% buffer containing 5% nonfat milk, and probed with specific antibodies in TBS-T buffer containing 5% nonfat milk or 5% bovine serum albumin according to manufacturer's instructions. Immunoblottings were performed using anti-gsk3β (1:500) (from Life technologies), anti-p-gsk3β^{Ser9} (1:1000), anti-Akt (1:1000), anti-p-Akt^{Ser473} (1:1000), anti-Erk1,2 (1:1000), anti-p-Erk1,2$^{Thr202/Tyr204}$ (1:1000), anti-p21 (1:1000) (from Cell signaling), anti-β-actin (1:1500) (from Sigma–Aldrich), anti-Rb (Santa Cruz Biotechnology) (dilution 1:200), anti-pRb $^{Ser249/Thr252}$ (Santa Cruz Biotechnology) (dilution 1:200), and rabbit polyclonal α-tubulin antibody (Sigma–Aldrich) (dilution 1:5000). Immunoreactive proteins were revealed by enhanced chemiluminescence (ECL) and semi-quantitatively estimated by Image Quant LAS 4000. Normalization was carried out with respect to the amount β-actin in the same sample. Alternatively, bands were visualized with autoradiography film, measured densitometrically and their relative density calculated based on the density of the α-tubulin band in each sample.

6.3. Computational methods

6.3.1. MD and DFT methods

First of all the molecules undergone a preliminary protocol in the framework of the Molecular Mechanics (MM), consisting of 1000 iterations of geometry optimization followed by 400 ns MD simulation at 298 K. A further 100 ns MD simulation was run to sample, randomly, ten structures which were subsequently optimized by means of first principle approach. Universal Force Field[32] was adopted to perform MM approach. On the other hand hybrid B3LYP[33–35] functional was applied in DFT calculation using the 6–311+G** basis set.[36,37] The Conductor-like polarizable continuum model (CPCM) [38–40] was adopted for calculating the solvent effect, for example, water. In this approach the solute molecule is embedded into a cavity surrounded by a dielectric continuum of a given permittivity and interacts with the solvent represented by a dielectric continuum model. Eventually Natural Bond Orbitals (NBO)[41] analysis was carried out in order to evaluate charge atomic charges and electrostatic potential maps.

6.3.2. VolSurf+ descriptors

The interaction of molecules with biological membranes is mediated by surface properties such as shape, electrostatic forces, H-bonds and hydrophobicity. Therefore, the GRID force field was chosen to characterize potential polar and hydrophobic interaction sites around target molecules by the water (OH_2), the hydrophobic (DRY), and the carbonyl oxygen (O) and amide nitrogen (N1) probe.[42] The information contained in the MIF (Molecular Interaction Fields) is transformed into a quantitative scale by calculating the volume or the surface of the interaction contours. The VolSurf+ procedure is as follows: (i) in the first step, the 3D molecular field is generated from the interactions of the OH_2, the DRY, O and N1 probe around a target molecule; (ii) the second step consists in the calculation of descriptors from the 3D maps obtained in the first step. The molecular descriptors obtained, called VolSurf+ descriptors, refer to molecular size and shape, to hydrophilic and hydrophobic regions and to the balance between them, to molecular diffusion, Log*P*, Log*D*, to the 'charge state' descriptors, to the new 3D pharmacophoric descriptors and to some descriptors on some relevant ADME properties. The definition of all 126 VolSurf+ descriptors is given in case studies with the old versions of VolSurf[43–48]; (iii) finally, chemometric tools (PCA,[49] PLS[50]) are used to create relationships of the VolSurf+ descriptor matrix with ADME properties. The scheme of the VolSurf+ program steps and a detailed definition of VolSurf+ descriptors have recently been reported.[29]

Acknowledgment

The authors are grateful to the Italian M. I. U. R. for the financial support.

References and notes

1. Levine, A. J. *Cell* **1997**, *88*, 323.
2. Moller, M. B. *Leuk. Lymphoma* **2000**, *39*, 19.
3. Tonani, R.; Bindi, S.; Fancelli, D.; Pittala, V.; Varasi, M. (2004), WO 2004013146 A1 20040212.
4. Tian, Y.; Wan, H.; Tan, G. *Oncol. Lett.* **2012**, *4*, 601.
5. Tonani, R.; Bindi, S.; Fancelli, D.; Pittala, V.; Danello, M. (2004), WO 2004007504 A1 20040122.
6. Malumbres, M. *Cancer Cell* **2012**, *22*, 419.
7. Barraja, P.; Caracausi, L.; Diana, P.; Spano, V.; Montalbano, A.; Carbone, A.; Parrino, B.; Cirrincione, G. *ChemMedChem* **2012**, *7*, 1901.
8. Diana, P.; Stagno, A.; Barraja, P.; Carbone, A.; Parrino, B.; Dall'Acqua, F.; Vedaldi, D.; Salvador, A.; Brun, P.; Castagliuolo, I.; Issinger, O. G.; Cirrincione, G. *ChemMedChem* **2011**, *6*, 1291.
9. Diana, P.; Carbone, A.; Barraja, P.; Kelter, G.; Fiebig, H.; Cirrincione, G. *Bioorg. Med. Chem.* **2010**, *18*, 4524.
10. Fortuna, C. G.; Forte, G.; Pittalà, V.; Giuffrida, A.; Consiglio, G. *Comput. Theor. Chem.* **2012**, *985*, 8.
11. Sorrenti, V.; Guccione, S.; Di Giacomo, C.; Modica, M. N.; Pittalà, V.; Acquaviva, R.; Basile, L.; Pappalardo, M.; Salerno, L. *Chem. Biol. Drug Des.* **2012**, *80*, 876.
12. Bindi, S.; Fancelli, D.; Alli, C.; Berta, D.; Bertrand, J. A.; Cameron, A. D.; Cappella, P.; Carpinelli, P.; Cervi, G.; Croci, V.; D'Anello, M.; Forte, B.; Laura Giorgini, M.; Marsiglio, A.; Moll, J.; Pesenti, E.; Pittalà, V.; Pulici, M.; Riccardi-Sirtori, F.; Roletto, F.; Soncini, C.; Storici, P.; Varasi, M.; Volpi, D.; Zugnoni, P.; Vianello, P. *Bioorg. Med. Chem.* **2010**, *18*, 7113.
13. Pevarello, P.; Fancelli, D.; Vulpetti, A.; Amici, R.; Villa, M.; Pittalà, V.; Vianello, P.; Cameron, A.; Ciomei, M.; Mercurio, C.; Bischoff, J. R.; Roletto, F.; Varasi, M.; Brasca, M. G. *Bioorg. Med. Chem. Lett.* **2006**, *16*, 1084.
14. Longo, A.; Brasca, M.G.; Orsini, P.; Traquandi, G. Pittala, V.; Vulpetti, A.; Varasi, M.; Pevarello, P. (2001), WO 2001098299 A1 20011227.
15. Musumarra, G.; Barresi, V.; Condorelli, D. F.; Fortuna, C. G.; Scirè, S. *Comput. Biol. Chem.* **2005**, *29*, 183.
16. Pittalà, V.; Romeo, G.; Materia, L.; Salerno, L.; Siracusa, M. A.; Modica, M.; Mereghetti, I.; Cagnotto, A.; Russo, F. *Farmaco* **2005**, *60*, 731.
17. Patanè, E.; Pittalà, V.; Guerrera, F.; Salerno, L.; Romeo, G.; Siracusa, M. A.; Russo, F.; Manetti, F.; Botta, M.; Mereghetti, I.; Cagnotto, A.; Mennini, T. *J. Med. Chem.* **2005**, *48*, 2420.
18. Schlemmer, H. P. *Radiology* **2008**, *48*, 45.
19. Jemal, A.; Siegel, R.; Xu, J.; Ward, E. *CA Cancer J. Clin.* **2010**, *60*, 277.

20. Alifrangis, C.; O'Hanlon-Brown, C.; Tuthill, M.; Waxman, J. *BJU Int.* **2012**, *109*, 1801.
21. Majumder, P. K.; Sellers, W. R. *Oncogene* **2005**, *24*, 7465.
22. Lin, H. P.; Jiang, S. S.; Chuu, C.-P. *PLoS One* **2012**, *7*, e31286.
23. Davis, R.; Singh, K. P.; Kurzrock, R.; Shankar, S. *Oncol. Rep.* **2009**, *22*, 1473.
24. Wu, Z.; Sun, H.; Zeng, W.; He, J.; Mao, X. *PLoS One* **2012**, *7*, e45825.
25. Royuela, M.; Arenas, M. I.; Bethencourt, F. R.; Sánchez-Chapado, M.; Fraile, B.; Paniagua, R. *Eur. Cytokine Network* **2001**, *12*, 654.
26. Uchida, C. *Curr. Drug Targets* **2012**, *13*, 1622.
27. Fortuna, C. G.; Barresi, V.; Musumarra, G. *Bioorg. Med. Chem.* **2010**, *18*, 4516.
28. Fichera, M.; Fortuna, C. G.; Impallomeni, G.; Musumarra, G. *Eur. J. Org. Chem.* **2002**, *1*, 145.
29. Fortuna, C. G.; Barresi, V.; Berellini, G.; Musumarra, G. *Bioorg. Med. Chem.* **2008**, *16*, 4150.
30. Doddareddy, M. R.; Cha, J. H.; Cho, Y. S.; Koh, H. Y.; Yoo, K. H.; Kim, D. J.; Pae, A. N. *Bioorg. Med. Chem.* **2005**, *13*, 3339.
31. Cruciani, G.; Miniconi, M.; Carosati, E.; Zamora, I.; Mannhold, R. In *Drug Bioavailability*; Wiley-VCH, 2004; pp 410–420.
32. Rappé, A. K.; Casewit, C. J.; Colwell, K. S.; Goddard, W. A.; Skiff, W. M. *J. Am. Chem. Soc.* **1992**, *114*, 10024.
33. Becke, A. D. *Phys. Rev. A* **1988**, *38*, 3098.
34. Lee, C.; Yang, W.; Parr, R. G. *Phys. Rev. B* **1988**, *37*, 785.
35. Becke, A. D. *J. Chem. Phys.* **1993**, *98*, 5648.
36. McLean, A. D.; Chandler, G. S. *J. Chem. Phys.* **1980**, *72*, 5639.
37. Krishnan, R.; Binkley, J. S.; Seeger, R.; Pople, J. A. *J. Chem. Phys.* **1980**, *72*, 650.
38. Klamt, A.; Schüürmann, G. *J. Chem Soc., Perkin Trans. 2* **1993**, *5*, 799.
39. Cossi, M.; Rega, N.; Scalmani, G.; Barone, V. *J. Comput. Chem.* **2003**, *24*, 669.
40. Takano, Y.; Houk, K. N. *J. Chem. Theory Comput.* **2005**, *1*, 70.
41. Foster, J. P.; Weinhold, F. *J. Am. Chem. Soc.* **1980**, *102*, 7211.
42. Carosati, E.; Sciabola, S.; Cruciani, G. *J. Med. Chem.* **2004**, *47*, 5114.
43. Cruciani, G.; Crivori, P.; Carrupt, P. A.; Testa, B. *J. Mol. Struct. Theochem* **2000**, *503*, 17.
44. Crivori, P.; Cruciani, G.; Carrupt, P. A.; Testa, B. *J. Med. Chem.* **2000**, *43*, 2204.
45. Cruciani, G.; Meniconi, M.; Carosati, E.; Zamora, I.; Mannhold, R. *Methods Principles Med. Chem.* **2003**, *18*, 406.
46. Berellini, G.; Cruciani, G.; Mannhold, R. *J. Med. Chem.* **2005**, *48*, 4389.
47. Mannhold, R.; Berellini, G.; Carosati, E.; Benedetti, P. In The Molecular Interaction Fields, edited b.
48. Cruciani, G.; Mannhold, R.; Kubinyi, H.; Folkers, G. series eds. Wiley-VCH Verlag GmbH & Co. KGaA, Weinheim, 2006, 27, 173.
49. Wold, S.; Sjöström, M. *ACS Symp. Ser.* **1977**, *52*, 243.
50. Wold, S.; Albano, C.; Dunn, W. J., III; Edlund, U.; Esbensen, K.; Geladi, P.; Hellberg, S.; Johansson, E.; Lindberg, W.; Sjöström, M. *NATO ASI Ser. Ser. C: Math. Phys. Sci.* **1984**, *138*, 17.